FTD-ID(RS)T-0752-82

FOREIGN TECHNOLOGY DIVISION

AIR FORCE SYSTEMS COMMAND

PHYSICS

(Selected Articles)

FOREIGN TECHNOLOGY DIVISION

Approved for public release;
distribution unlimited.

EDITED TRANSLATION

FTD-ID(RS)T-0752-82 1 November 1982

MICROFICHE NR: FTD-82-C-001399

PHYSICS (Selected Articles)

English pages: 34

Source: Wuli, Vol. 10, Nr. 11, November 1981,
pp. 654-660; 666-671

Country of origin: China
Translated by: LEO KANNER ASSOCIATES
F33657-81-D-0264
Requester: FTD/TQTD
Approved for public release; distribution unlimited.

THIS TRANSLATION IS A RENDITION OF THE ORIGINAL FOREIGN TEXT WITHOUT ANY ANALYTICAL OR EDITORIAL COMMENT. STATEMENTS OR THEORIES ADVOCATED OR IMPLIED ARE THOSE OF THE SOURCE AND DO NOT NECESSARILY REFLECT THE POSITION OR OPINION OF THE FOREIGN TECHNOLOGY DIVISION.	PREPARED BY: TRANSLATION DIVISION FOREIGN TECHNOLOGY DIVISION WP-AFB, OHIO.

Table of Contents

Graphics Disclaimer ii

Advances in Chemical Lasers, by Luo Jingyuan and Hu Shiheng 1

Advances in Research on Solid Optical Thin Film Structures,
by Zhong Yongan 19

GRAPHICS DISCLAIMER

All ures, graphics, tables, equations, etc. merged into is translation were extracted from the best quality copy available.

Advances in Chemical Lasers

by Luo Jingyuan and Hu Shiheng
(The Dalian Chemicophysics Institute, Chinese Academy of Sciences)

Chemical lasers are a new area of lasers developed on the fringes of chemistry and physics. It involves research of the chemical kinetics of unbalanced reactions, the gas kinetics of reaction flows and the laser physics of high gain mediums. Because of the mutual integration of these subjects, since the first chemical laser appeared in 1965, there have been tremendous advances in chemical lasers and these have attracted the attention of many.

The first chemical laser relied on the following reaction pump:

$$H + Cl_2 \rightarrow HCl\ (v \leqslant 6) + Cl \qquad (1)$$

This reaction produces an excitation state of HCl on each vibration level of the high attained $v \leqslant 6$ and uses the pulse method to transmit a 3.7-4.0 micrometer ultraviolet laser. Later, they also discovered many other laser systems such as the HF (DF), HBr (DBr), CO, $DF-CO_2$ and iodine atomic. Among these, the iodine atomic laser has the shortest wavelength, 1.315 micrometers, and the longest system is the pure rotation jumping HF laser.

Early chemical laser components were only able to operate with the pulse method; efficiency was low and output was small. They were mainly used as implements for studying chemical reaction kinetics. Since the 1970's, owing to aerodynamic technology introducing the continuous wave laser as well as

relativistic ion beam initiation technology introducing pulsed lasers, chemical lasers have made great breakthroughs. In one leap they have become high power and high energy devices which have been given a good deal of attention. It has been reported that the continuous wave HF(DF) laser has attained output power of 400,000 watts [2] and the pulsed HF laser oscillator has attained single pulse output energy of 4.2 kilo-joule [3]. This laser has had the highest output power (continuous wave device) to date. Moreover, the electrooptic efficiency which has reached 900% (pulsed HF laser with relativistic electron beam initiation) is the highest efficiency pulsed device. As a result, chemical lasers have become the most hopeful means of realizing laser weapons and for possible use in the area of laser nuclear fission. At the same time, many research laboratories have gradually begun to use chemical lasers for studying basic problems in various new types of chemistry and physics. These include the chemical reactions of specific condition molecules and the energy shift process as well as their relation with the operating performances of chemical lasers. This is an important aspect of chemical laser research work.

Below we will divide the chemical laser into vibration-rotation, electron jumping and pure rotation based on the jumping modes of the chemical laser vibration and discuss each mode individually.

I. The Vibration-Rotation Jumping Chemical Laser

The majority of existing chemical laser systems are vibration-rotation jumping. The HF(DF) and CO lasers have become especially advanced.

We know that the basic principle of chemical lasers [4-6]

is reliance on the chemical reactions realizing particle number reversal. Thus, the energy released by the chemical reaction transforms into coherent laser energy. As a result, in order to obtain a chemical laser, it is first required that the chemical reaction be an exothermic reaction. Second, the energy released by the chemical reaction must be selected and distributed to each internal energy state of the reaction products to form particle number reversal. That is, the reaction product is an athermal balance (non-Boltzman) distribution on each of its internal energy states. For example, the HF system first discovered by Kompa and Pimentel [7] has a pump reaction of:

$$F + H_2 \rightarrow HF(v \leqslant 3) + H + 132 \text{ kilojoule/mole} \qquad (2)$$

Tests measured that the energy released by the reaction was 132 kilojoule/mole and the rate of distribution for the vibration, rotation and mean motion was -0:66:0.08:0.26. That is. 66% of the energy transformed into vibratory energy and the distribution rate of this vibratory energy on each energy level v=3,2,1 was 0.47:1.00:0.29. Moreover, during the initial period of the reaction there appeared to be no HF with v=0 produced. We can see the particle number reversal produced within each energy level v=2,1,0 (see fig. 1) and before this reversal distribution was lost because of particle collision relaxation, there was $v-2 \rightarrow 1$ and $v=1 \rightarrow 0$ jumping and a chemical laser was simultaneously produced in two vibration bands

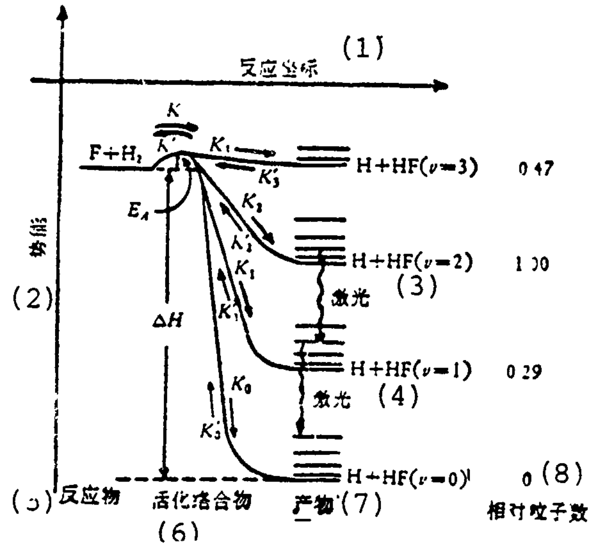

Fig. 1 The Reaction Coordinates of HF(v) Produced on Each Vibration State in the F + $H_2 \rightarrow$ HF(v) + H Reaction

Key: 1. Reaction coordinates
2. Potential energy
3. Laser
4. Laser
5. Reactant
6. Active complex compound
7. Product
8. Relative particle number

1. The HF(DF) and CO Continuous Wave Chemical Laser

The HF(DF) and CO chemical laser has advanced into a high powered continuous wave device.

The high powered HF(DF) laser usually relies on reaction formula (2) or two reaction formulas (2) and (3) for pumping F.N.1):

$$H + F_2 \rightarrow HF\ (v \leq 9) + F + 410\ \text{kilojoule/mole} \qquad (3)$$

F.N.1) Reaction formula (2) is commonly called the "cold reaction and reaction formula (3) is called the "hot" reaction

The various pump reactions of excitation HF(v) are generally initiated by F atoms. The reaction is:

$$NO + F_2 \rightarrow NOF + F \qquad (4)$$

It provides a simple path for producing F atoms from bottled gas. However, a combustion chamber is commonly used in the high powered continuous wave HF(DF) device [6,8] to produce F atoms (see fig. 2).

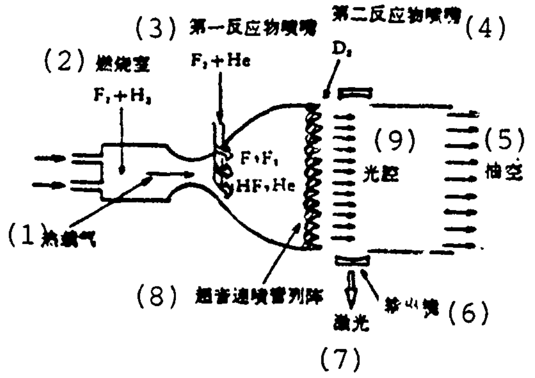

Fig. 2 Schematic of the Supersonic Continuous Wave Chemical Laser [8]

Key: 1. Heat carrier gas
2. Combustion chamber
3. First reactant jet
4. Second reactant jet
5. Air bleed
6. Output mirror
7. Laser
8. Supersonic nozzle array
9. Optical cavity

The reason for this is that the dissociation energy of the F_2 is relatively low (157 kilojoule/mole) and when a high exothermic F_2-H_2 chain reaction takes place, a high temperature can be maintained in the combustion chamber. As a result, this causes an additional excess of F_2 which is totally dissociated. Thereafter, the high temperature, high pressure gas mixture is expanded by the supersonic nozzle array. It enters the reaction chamber (the optical cavity in fig. 2) and the expansion can

cause the gas to cool and freeze the required F atoms. This main gas flow quickly combines with the second reactant gas flow (D_2 in fig.2)[1] and produces a pump reaction. In this type of device, the optical axis is opposite the gas flow and assumes a transverse position. Tests have attained continuous wave DF laser outputs greater than 40,000 watts.

We know that in order to obtain F atoms, we must dissociate the F_2 or fluoride under a high temperature; and to maintain particle number reversal and effective excitation transmission, the pump reaction will also need to be carried out under a low temperature. Use of a supersonic nozzle effectively resolved this problem. Usually, the gas temperature entering the nozzle's inlet is about 1,500-2,000K and after expansion the temperature in the area of the optical cavity drops to room temperature. Aside from this, under several torr pressure, although the speed of the HF(DF) pump reaction is fast, relaxation is also very fast. According to statistics, we must produce a laser effect in a microsecond time quantity and exhaust the medium from the resonant cavity to be able to attain high output power. After the main gas flow in the combustion chamber is expanded by the supersonic nozzle, the gas pressure is only several torr in the optical cavity and the speed reaches (2-4) x 10^5 centimeters$\cdot$second^{-1}. This guarantees that the gas flow will pass the optimal cavity within a microsecond time quantity. Moreover, the supersonic nozzle can also cause the F atoms produced in the combustion chamber to "freeze" so that they participate in the pump reaction of the optical chamber. We can see from this that the supersonic nozzle has a key function in the continuous wave chemical laser.

A great deal of attention has also been given to the high powered CO chemical laser. The work of Wiswall and others [9] has brought about great advances in the CO laser. In a high temperature combustion chamber ($>$ 2,500K) they used

F.N. 1) If the HF laser is used, then H_2 can substitute for D_2. D_2H_2 is sprayed in by small nozzles between the main transonic nozzles.

NF_3-CH_4-H_2-CS_2 as the material and pyrolysis produced the CS and S components needed for pump reaction formulas (5) and (6). Further, by properly controlling the CS/CS_2 and CS/S ratios in the combustion chamber they could guarantee that the O atoms could not be consumed in great quantity by reaction formula (7) and cause the entire CS to transform into CO(v):

$$S + O_2 \rightarrow SO + O + 23 \text{ 千焦耳/摩尔}^{(1)} \quad (5)$$

$$O + CS \rightarrow CO(v \leqslant 15) + S + 356 \text{ 千焦耳/摩尔}^{(2)} \quad (6)$$

$$CS_2 + O \rightarrow SO + CS \quad (7)$$

Key: 1. Kilojoule/mole
2. Kilojoule/mole

At present, because the attained 0.5 kilowatt continuous laser power resolved the key technical problems, technologically there are no great obstructions to this device expanding its range.

One important reason why the CO laser has gained serious attention is that the collision and vibration relaxation of CO molecules are much slower than those of the HF(DF). Therefore, the CO can possibly operate under high optical cavity pressure (about 40-50 torr) and the activation area length (about 30 centimeters) is obviously advantageous in the HF(DF) system.

It should be pointed out that reaction formulas (2), (3) and (6) are mainly used in pumped high powered continuous wave devices. Although the F_2-H_2 system possesses obvious superiority, yet the toxicity of F_2 is great and is difficult to handle. Various other types of initial gas mixtures and

pump reactions [6,8] are often used in small HF(DF) and CO devices. For example, the small HF laser can use SF_6 as the fluorine source and only relies on cold reaction formula (2) for pumping.

2. The Pulsed HF Laser With Electron Beam Initiation

The pulsed chemical laser has many types of initiation methods. For example, by using flash photolysis or gas electric discharge for the production of F atoms to initiate pump reaction, it is easy to attain low power pulsed vibration. Yet efficiency is low and output small. In order to produce short pulses in the HF and other pulsed devices, it is necessary to raise the pressure and accelerate the reaction. At the same time, because HF etc. haloid acid molecule vibration relaxation is very fast, it is also necessary to have rapid initiation. Therefore, in recent years, HF pulsed lasers which take high power as the goal use relativistic electron beam initiation technology.

Gerber and others used the device shown in fig. 3.

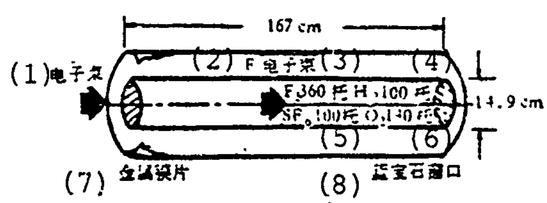

Fig. 3 Schematic of the Pulsed HF Laser With Relativistic Electron Beam Initiation

Key: 1. Electron beam
2. E electron beam
3. Torr

Key: 4. Torr
5. Torr
6. Torr
7. Metallic diaphragm
8. Sapphire window

Fill 360 torr F_2, 100 torr SF_6, 100 torr H_2 and 140 torr O_2 into a stainless steel tube with a length of 167 centimeters and a diameter of 14.9 centimeters. Insert a 2 megaelectron volt relativistic electron beam from the metallic diaphragm surface and from the laser pulse of the facing sapphire window with output energy of 2.4 kilojoule. The pulse width is 35 millimicroseconds and the electrical efficiency (relative to the absorbed electron beam energy) is 180%. Before long, this device is lengthened to 2.3 meters. Then it could attain pulse output of 4.2 kilojoule, electrical efficiency was 200%, chemical efficiency was 10% and the pulse width was 26 millimicroseconds [3]. Afterwards, they used a similar device which could use a 2 megaelectronvolt accelerator for initiation. It attained a 4.2 kilojoule single pulse output, pulse width was 20 millimicroseconds, chemical efficiency was 11.4%, electrical efficiency was 180%, light beam divergency (using an unstable cavity) was 4 milliradian and its peak power reached 100 kilo-megawatts. The key to causing the laser energy to greatly increase lies in greatly raising the reaction speed by electron beam initiation. At the same time, they fully use the potential force of chain reaction formulas (2) and (3). Foreign nations are actively researching the use of this type of laser in laser nuclear fission. For this reason, it is necessary to further compress the pulse width to under 1 millimicrosecond. Yet, it is feared that compressing it to under a submillisecond is difficult.

3. Advances in Other Vibration-Rotation Jumping Lasers

When compared to the HF(DF) and CO high powered lasers, to date other continuous wave chemical lasers have only been

able to give medium power. Arnold and others [10] used chemical initiation and obtained watt level continuous wave output from HCl and HBr lasers. Both of these devices depend on NO and ClO_2 reactions to produce Cl atoms. The total chemical process is complex yet it must depend on the pump reaction

$$Cl + HI \rightarrow HCl\ (v \leqslant 4) + I + 132\ \text{kilojoule/mole} \quad (8)$$

It is necessary to use sufficient Cl atoms to completely realize the laser effect.

Hu Shiheng and others [11] have proposed an advanced plan which uses the

$$F + Cl_2 \rightarrow ClF + Cl \quad (9)$$

reaction, that is, in engineering, it is easy to attain the F atoms to produce the required large number of Cl atoms. Tests have proven the feasibility of this plan thus providing a possible amplified high powered HCl chemical laser plan.

In the HBr laser, it is first necessary to rely on added Br: to transform the Cl atoms into Br atoms. Then, after reacting with HI it produces vibration excited HBr(v):

$$Br + HI \rightarrow HBr(v \leqslant 2) + I + 68\ \text{kilojoule/mole} \quad (10)$$

However, the power of this type of HBr laser system is very low. Recently, Hu Shiheng and others proposed a possible amplification plan. It uses reaction formula (2) to easily transform the F atoms produced in engineering into the required H atoms. Afterwards, from the pump reaction

$$H + Br_2 \rightarrow HBr(v \leq 6) + Br + 173\ \text{kilojoule/mole} \quad (11)$$

there is produced vibration excited HBr atoms. Preliminary tests proved that this plan is feasible and it can operate at high power.

There are many uses for the various small scale continuous

wave chemical lasers. For example, the small HF continuous wave device acts as a search laser which can diagnose high powered large scale devices. Hinchen and others [12] used the HF laser in infrared double resonance tests and to research the rotation and relaxation of HF. The pulsed chemical laser with moderate energy can also be used to study the problems of the shift of vibration energy. Much work has already been done in this area, yet many problems are still unresolved; determining the speed of various free atom relaxation and determining the relaxation speed of each high vibration energy level ($v > 1$) is especially difficult. At present, these problems are still being studied.

In recent years, there has been a great deal of attention given to infrared lasers in laser chemistry especially the prospects of its application in the area of the laser separation of isotopes. At present, special attention is being focused on the isotopic separation of UF_6 and other uranium chemical compounds. The vibration-rotation spectral line of the ν_3 modulus is in the proximity of 16 micrometers. This impelled people to develop a new type of laser with a 16 micrometer wave band. It appears that chemical lasers can very possibly be applied in this area. Osgood [13] used the HBr laser and CO_2 laser to simultaneously irradiate a HBr-CO_2 mixed gas (about 0.5-7 ton) and obtained a 16 micrometer laser. Very recently, for this aim, Rutt [14] also made an anticorrosive pulsed HBr laser which is easily safeguarded. Every pulse can put out 550 millijoule of energy.

II. The Electron Jumping Chemical Laser

In recent years, a great deal of attention has been given to the electron jumping chemical laser. The reason for this is that the electron jumping of atoms and molecules can transmit a 0.2 to 1 micrometer short wavelength laser. To date, many research articles have been published and it appears that

chemical pumps are the most advantageous for realizing continuous wave electron jumping lasers. However, a completely satisfactory electron jumping chemical laser has still not been found.

Recently, when Cool [8] commented on the difficulties of operating electron jumping lasers, he concluded that the following conditions must be satisfied in order to realize an electron jumping. Continuous wave chemical laser:

(1) The average radiation life of the laser energy level must be $\geqslant 10^{-5}$ seconds.

(2) The average collision life of the laser energy level must also be $\geqslant 10^{-5}$ seconds. When pressure is 1 torr, this indicates that the probability of the net collision eliminating activation will not exceed 10^{-2} and when operating under higher pressure this value should correspondingly drop.

(3) The concentration of each reactant should be $\geqslant 10^{15}$-10^{16} centimeters^3. Therefore, it is necessary to have effective measures for producing various types of atoms or free radicals.

(4) Pump reactions must be quick and the energy must be a highly unbalanced distribution so that the particle number distribution probability of the laser energy level's single excited energy level can be greater than 10^{-3}.

(5) The particle number distribution of the laser energy level must be minimum. In a low state which is a bound state, these particles can effectively relax collision or be eliminated from the optical cavity; if the low state is dissociated (e.g. the same as in the quasi-molecular laser system), this is even more ideal.

At present, the only successful device is the iodine atom electron jumping chemical laser developed by Bousek and others [15]. In tests, they used the simple chemical reactor

shown in fig. 4 which allows a chlorine air flow to use 90% H_2O_2 lye to produce excited metastable state $O_2^*(^1\Delta_g)$. They also used dry ice-alcohol cold well to collect water and other high melting point reactants. The $O_2^*(^1\Delta_g)$ gas escapes from the top of the reactor and is then that the non-reacting Cl_2 is eliminated by the cold well which has a temperature of $-154^{\circ}C$. The reactor's outflow substances and I_2 molecules combine in the inlet of the longitudinal flow laser cavity.

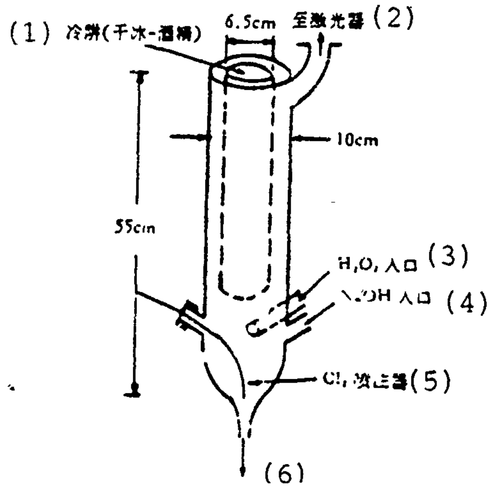

Fig. 4 Schematic of the Reactor Which Uses a Chemical Method to Produce $O_2^*(^1\Delta_g)$ in an Iodine Continuous Wave Chemical Laser [15]

Key: 1. Cold well (dry ice-alcohol)
2. To the laser
3. Inlet
4. Inlet
5. Injector
6. To the drain pipe

At this time, support is drawn from the energy shift of the metastable state so that the I_2 molecules dissociate and produce excitation state $I(^2P_{1/2})$ atoms. Finally, vibration is realized on $(^2P_{1/2}-^2P_{3/2})$ self-rotating-orbital jumping of the iodine atoms.

The transmitting wavelength of the infrared laser is 1.315 micrometers. Strictly speaking, this system belongs to the shift type chemical lasers because the high metastable state $O_2^*(^1\Delta_g)$ is still produced by a chemical reaction. Moreover, the resonant energy near the rear directional I atoms is used to realize radiation. The mechanism of this system for the most part includes the following several important steps:

$$O_2^*(^1\Delta_g) + O_2^*(^1\Delta_g) \rightarrow O_2^*(^1\Sigma_g^+) + O_2(^3\Sigma_g^-) \qquad (12)$$

$$O_2^*(^1\Sigma_g^+) + I_2 \rightarrow O_2(^3\Sigma_g^-) + 2I(^2P_{3/2}) \qquad (13)$$

$$O_2^*(^1\Delta_g) + I(^2P_{3/2}) \rightleftharpoons O_2(^3\Sigma_g^-) + I^*(^2P_{1/2}) \qquad (14)$$

$$I^*(^2P_{1/2}) + O_2^*(^1\Delta_g) \rightarrow O_2^*(^1\Sigma_g^+) + I(^2P_{3/2}) \qquad (15)$$

The four steps of the above mentioned mechanism are crucial because they can regenerate $O_2^*(^1\Sigma_g^+)$ and they can especially guarantee that I_2 can be totally dissociated. Otherwise, the remaining I_2 can cause the $I^*(^2P_{1/2})$ to eliminate activation.

This type of laser has developed very quickly and they have already attained over 100 watt continuous wave output power on a transverse flow device [16]. Based on calculations by Benard and others, it is possible to derive 600 watts of power from an existing device. Although the wavelength of this type of laser is relatively long, it cannot be tuned and is not the most ideal. Yet, it can produce high power and has thus attracted a great deal of attention.

Various nations are actively investigating electron jumping chemical lasers with visible and ultraviolet wave bands. However, there have not been any real breakthroughs.

III. The Pure Rotation Jumping Chemical Laser

Usually, energy is released by the chemical reaction. Although only a small portion transforms into the rotational energy of produced molecules yet initially the energy level of each rotation is possibly unequally distributed. For example, the energy released by reaction formula (2) has about 8% which transforms into rotational energy. Moreover, during the initial period of the reaction, the rotational energy is unequally distributed. Yet it is very difficult to obtain laser gain for the pure rotation jumping of the HF(v,j) low J value. The reason for this is that the pure rotation relaxation of the low J rotation state is very fast and the rotation reversal distribution created by the reaction will quickly decay into a thermal equilibrium distribution. To overcome this difficulty, the pump speed must be faster than the speed commonly attained by chemical reactions. For molecules such as HF, the rotation relaxation of their J states is quite slow and the rotation excited molecules are exceptionally stable. Moreover, the Einstein coefficient of the pure rotation jumping is quite large and as a result it is quite easy to attain pure rotation excitation [17].

In 1967 the first pure rotation jumping laser was reported [18] and in 1974 a rotation jumping laser with a pure chemical pump was developed. Yet, to date, only the HF [17-19] and OH (or OD) [20,21] are able to use this method to produce excitation. Moreover, among the rotation jumping which occurs in various very high rotational energy levels (see table 1) [22] - the specific mechanisms are discussed in detail in the above mentioned references - the speeds of many basis elements as well as their detailed mechanisms are unclear and thus still require more thorough research [17,19].

(1) 激光体系	(2) 泵浦反应	(3) 激光跃迁上能级		(5) 激光跃迁频率 (厘米$^{-1}$)	(6) 可能的泵浦机制
		v	(4) J 或 N		
HF	$CH_3 + CF_3 \longrightarrow CH_2 = CF_2 + HF$	0	17,18	659, 693	化学反应 (7)
HF	$CH_2 = CF_2 + h\nu \longrightarrow CH \equiv CF + HF$	0 1 2 3	12—14 13,14 14 15	48[illegible]—513 497, 513 511 502	光化学反应 (8)
OH	$O(^1D) + H_2 \longrightarrow OH + H$	0 1 2 3	8—20 10—22 10—23 10—19	326—723	化学反应,随即近共振 V-R 能量转移 (9)

Table 1 The Pure Rotation Jumping Chemical Laser

Key: 1. Laser system
2. Pump reaction
3. Laser jumping energy level
4. Or
5. Laser jumping frequency (centimeters^{-1})
6. Possible pump mechanism
7. Chemical reaction
8. Photochemical reaction
9. Chemical reaction, very close to energy shift of resonant V-R

This paper briefly discussed the development of chemical lasers, focusing on the HF(DF) as a representative high powered laser as well as the close relationship between chemical lasers and basic research in kinetics. It also discussed certain applications of the chemical laser. Other important aspects of the chemical laser such as problems in gas kinetics, optical resonant cavities and computer simulation were not discussed. References [5,6] made systematic summaries of each aspect regarding the chemical laser and these can be referred to by interested readers.

It appears that chemical lasers are still being quickly developed. At present, there are only two types of chemical lasers, the HF(DF) and CO. Development work on them is close

to completion and the next step is the development of large scale laser systems in engineering. At the same time it is necessary to actively investigate and develop various types of new chemical laser systems including short wavelength systems. This is needed to meet the multifaceted technical application requirements in laser weapons, laser nuclear fission and laser chemistry. Because chemical lasers completely or for the most part depend on chemical energy to obtain laser energy, it is expected that the development of various types of compact high energy chemical lâser devices will become the main candidates for laser weapons. It is expected that high powered chemical lasers will be widely applied in ground and ship antimissile, anti-aircraft, airborne antimissile and satellite antimissile technology. We believe that the development prospects of chemical lasers are vast and their prospects for use are encouraging.

References

[1] J.V.V. Kasper and G.C. Pimentel. Phys. Rev. Lett., 14(1965), 352

[2] Aviation Week and Space Techology, 113-5 (1980), 55.

[3] J.B. Gerardo, IEEE/OSA Conference on Laser Engineering and Applications. May, (1975).

[4] Luo Jingyuan, Nature Magazine, 2(1979), 351.

[5] K.L. Kompa, author, Luo Jingyuan, translator, Chemical Lasers, Science Press, (1981).

[6] Handbook of Chemical Laser, Ed.R.W.F. Grass. J.F. Bott J. Wiley and Sons, New York, (1976).

[7] K.L.Kompa and G.C. Pimentel. J. Chem. Phys., 47(1967).857.

[8] T.A. Cool, Physical Chemistry of Fast Reactions Vol.2: "Reaction Dynamics." Ed. I.W.M. Smith, 2 Chap. 3. Plenum Press, New York. (1979).

[9] W.Q.Jeffers. C.E. Wiswall et al., J. Appl. Phys. 49 (1978), 2509.

[10] S.J. Arnold et al., IEEE j. Quant. Electron., QE-14 (1978, 293.

[11] Hu Shiheng, Zhang Cunhao et.al., Lasers, 7(1980), 86.

References (continued)

[12] J.J. Hinchen. R.H. Hobbs. J. Chem. Phys., 65 (1976),2732.

[13] R.M. Osgood,Jr., Appl. Phys. Lett. 28(1976). 342.

[14] H.N. Rutt, J.Phys. D, 12(1979). 345

[15] W.E. McDermott et al., Appl. Phys. Lett., 32(1978).469

[16] D.J. Benard et al., Appl. Phys. Lett. 34(1979).40.

[17] J.J. Hinchen and R.H. Hobbs, J.Appl. Phys., 50(1979).628

[18] T.F. Deutsch. Appl. Phys. Lett.11(1967).18.

[19] E. Cuellar, G.C. Pimentel. J.Chem. Phys. 71(1979). 1385.

[20] G.D. Downey. D.W. Robinson. J.H. Smith. J. Chem. Phys., 66(1977). 1685.

[21] J.H.Smith, D.W. Robinson. J. Chem. Phys.,68(1978). 5474

[22] I.W.M. Senith, Optics and Laser Technology, 12(1980).77.

Advances in Research on Solid Optical Thin Film Structures

by Zhong Yongan
(Physics Department, Teacher's College of Shaanxi)

I. Preface

When solid optical thin film is mentioned, most of the time it refers to thin film prepared by the vacuum evaporation method. It is also the so-called physical steam sedimentation film. The preparation process of this type of thin film is influenced by many conditions. For example, because the factors of evaporation materials, heating raw materials, evaporation speed, environmental conditions, basic materials and basic temperature are different, the qualities and structures of the formed thin films are also different. Moreover, theoretical calculations often greatly differ from the results of actual measurements. These are the so-called multiple changes of the multiple factors influencing the thin film when the film is forming. It is not easy to prepare a type of thin film which conforms to the requirements and also has long endurance. Therefore, to develop an optical thin film which conforms to the requirements is an important topic in the study of thin film structures.

Early analysis of the quality of thin films tended to emphasize physical characteristics testing and chemical component analysis. Because test conditions are limited in form analysis, at the beginning only observations with an optical microscope could be relied on until the appearance of the electron microscope. Then, greater understanding was gained of the structure and form of the think film's surface. In 1966,

Pashly [1] used an electron microscope to observe the formation of the nucleus and growth of the thin film. During growth the structure rapidly changed. He used a movie camera to film it and obtained important materials. In the same year, Grigson and Dove [2] made further evaporations and observations on the growth and form of thin film in a diffractor equipped with a scanning device.

Following the expanded application of thin solid film, especially in the area of optical thin film, there was a daily increase of plating components with multilayered film systems because of the rapid development of laser technology. This posed even higher demands on the quality of the film especially in regard to reliability and endurance. However, during the production and application process, for one type of phenomenon such as the problem of the red shift of narrow band optical filter, explanation was often difficult. This caused people to carry out further research on the internal structure of thin film.

This paper only deals with several aspects of the most important advancements in solid optical thin film, structural research, briefly presents research methods and presents problems which need to be discussed.

II. The Multiporous Structure of Thin Film

In an article written in 1970 [3], Pearson introduced the composite technique which uses the transmission electron microscope. First, pictures were taken of the microscopic structure of the multilayered thin film's cross section. This was an important advancement in solid thin film research during the 1970's.

Pearson photographed samples with multilayered film systems. Among them was the thin film with a total medium

Fabry-Perot filter. Fig. 1 is an electron microscopic photo of a cross section of this type of film system. The thin film has a columnar structure and the crystals have columnar growth.

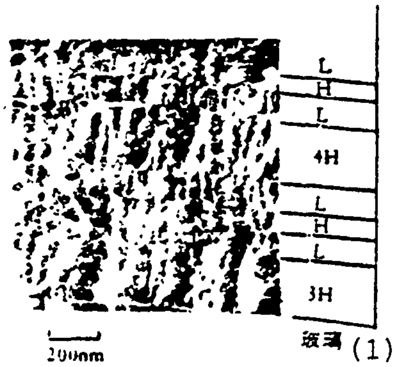

Fig. 1 Electron Microscopic Photo of a Cross Section With a Total Medium Fabry-Perot Filter

H is the high refracting power n=2.35 zinc sulfide film layer; L is the low refracting power n=1.35 cryolite film layer.

Key: 1. Glass

Aside from the columnar bodies in the thin film, the other parts are spaced. The columnar bodies seem to grow vertical to the bottom surface. There is a noticeable boundary line between the layers and the lower level crystal does not continuously grow with the upper layer crystal but a distance is erroneously opened. This also reveals that the space in the lower layer is not completely joined with the upper layer. This special characteristic has caught the interest of many and much attention has been given to the close relationship between the thin film's structure and many optical characteristics (e.g. refracting power, transmissivity and optical scattering).

The key as to whether we can actually show the columnar

structure of the film layer lies in the composite technique of making transmission electron microscope samples. Fig. 2 is a schematic of a broken off cross section of a film layer. In the figure, S_{c_1} and S_{c_2} are the directions of the carbon maintained film evaporation and S_p is the platinum preformed negative direction.

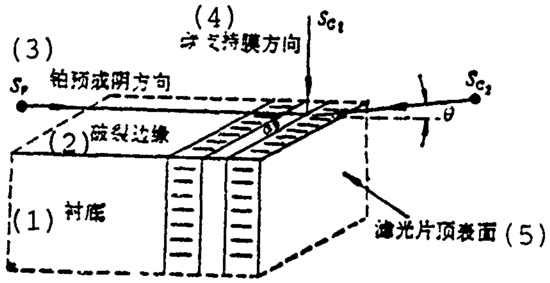

Fig. 2 Schematic of a Broken Off Cross Section of Thin Film

Key: 1. Substrate
2. Broken off boundary
3. Platinum preformed negative direction
4. Carbon maintained film direction
5. Top surface of filter

1. Infiltration Pattern of Water Vapor in Thin Films

In 1976, MacLeod and Richmond researched the effects of humidity permeating the filter and discovered that thermal treatment caused changes in the film layer. They also introduced changes by test patterns to observe the level of humidity permeation (see fig. 3 [4].

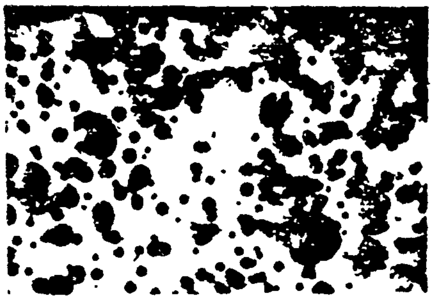

Fig. 3 Pattern of Humidity Permeating MgF_2/ZnS Filter. The White Section in the Figure is the Permeated Humidity

The work by MacLeod and others was an advancement following Pearson's discovery of the "columnar body + hole" structures. They found humidity permeation holes in the thin film so that the holes became humidity permeation and entrenched spaces. When the humidity penetrates into the holes this increases the refracting power of the thin film. Because the refracting power of the empty holes is 1 and the refracting power of the water is 1.33, this causes the optical thin film thickness to enlarge. This test observation very strongly shows that the "red shift" of the narrow band filter's peak value wavelength mainly comes from the permeation of the water vapor in the atmosphere on the filter (see fig. 4).

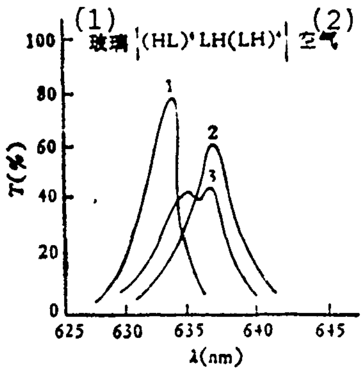

Fig. 4 Characteristics of the Shift (Red Shift) of the Narrow Band Zinc Sulfide and Cryolite Filter

1 is the charactcristic curve of the just made filter;

2,3 are separately the characteristic curves of the filter after 3 days and 4 days.

Key: 1. Glass
2. Air

After analysis of the measurement results of many thin films, it was discovered that the permeation speed and permeation depth of humidity for magnesium fluoride must be much greater than that for cryolite. I think that the magnesium fluoride film layer has high anti-tensile stress and has small fine cracks so that the humidity permeates the entire film layer along these cracks very quickly.

MacLeod and others also mentioned that after the filter is completed it is put aside for 11 minutes. Then, it is heated in a vacuum to 200°C and the humidity is driven out. A high temperature is maintained for 4 hours, later dropped to room temperature and finally it is exposed to air. This type of heat process technique is effective for the characteristics of a stable filter. The major result is the prevention of humidity

permeation.

In a visible light area, the materials generally used for narrow band filters are zinc sulfide, cryolite or magnesium fluoride. If a thin film of these materials is close to room temperature, it then collects and forms columnar bodies. The micropores in the film layer are very easily filled with water vapor and thus the refracting power and optical thickness of the thin film increase. The situation for multilayered film is even more complex. The outer layer is like a single layer film. Afterwards, the water vapor very quickly permeates to the second layer until it permeates to the bottom and other layers of the thin film. The material in the spaces between the layers is neither the same nor joined. The speed of water vapor permeation is closely related to the film material, vapor plating, the film system structure and environmental humidity. Thus, the "red shift" of the narrow band filter also has randomness.

MacLeod and others also discovered that the large micropores in the film layer are very possibly defects created by dirt. Material can also be provided on multilayered medium film structural changes after studying the humidity penetration patterns.

Studies have shown that the internal factor of the λ_0 shift is the porous structure of the film layer and the external factor is the permeation of the humidity. As regards the multilayered film, the humidity permeation process is very complex and does not uniformly permeate the entire surface. However, it does transversely spread into the film layer by means of these radii which are micropores with certain critical values. Therefore, the size of the micropores is directly related to the speed of the humidity permeation. This

involves the quantitative measurement of the film's aggregation density and the size of the micropores.

2. The Aggregation Density of Thin Film

We know that lead oxide thin film is extremely unstable in photoconduction thin film and is a type of film which easily changes. In 1966, Drift [5] of Holland used a transmission electron microscope to photograph a cross section of this type of thin film. It can be seen very clearly from the photos that the lead oxide crystallite in the thin film grew vertically on the substrate and possessed a needle shaped structure.

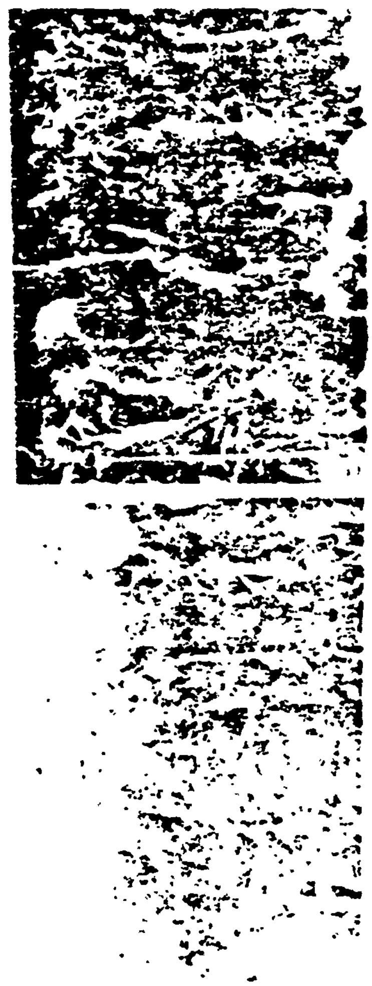

Fig. 5

Fig. 5 Photograph of a Cross Section of Lead Oxide Film With an Electron Microscope

(a) One side close to the glass substrate;

(b) One side close to the thin film's surface.

The lead oxide is prepared by the vacuum evaporation sedimentation method. However, it has a special technique which requires the permeation of a certain quantity of oxygen and water vapor during the steam coating process. Thus, the water component in this type of film layer is known in advance. In Drift's article, although the term "columnar body" did not exist at the time, he expressed the porous characteristics within the thin film. Fig. 6 shows how the cross section in the lead oxide film was photographed. The right side is the contact portion with the substrate and the left side is the film layer surface facing the steam source portion.

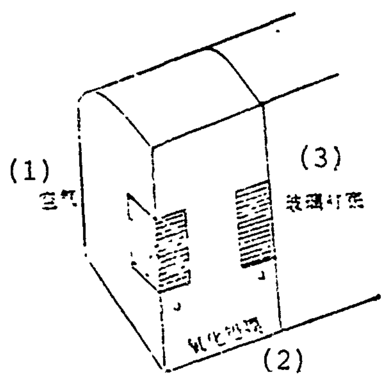

Fig. 6 Schematic of a Cross Section of a Lead Oxide Thin Film

Key: 1. Air
2. Lead oxide film
3. Glas substrate

Drift used the Brunaner, Emimett and Teller method (abbreviated as the B.E.T. method) to measure the prosity of the film layer. That is, he employed the absorption which

uses an inert krypton gas single molecule layer to measure and calculate 50% of the porosity. He measured the total surface of the crystal as about $50m^2/g$ and after calculating the mean thickness of the crystal as about 50 Å, the size of the crystal was $2\mu m \times 0.5\mu m$. The growth direction of the crystal showed an obvious tendency to be determined by the lead oxide steam molecule angle of incidence. This tendency was created by the film's selectivity in the gradual formation during the sedimentation process.

In the area of medium film, when Ogura [6] and MacLeod analyzed the absorption of water in optical thin film in 1976, they specially used the parameters of the aggregation density to explain the effects of water vapor. Moreover, they especially considered the distribution of the inner surface area and the micropore size. They used the theory of the absorption isothermal line proposed by Wheele as the basis. This hypothesis joined the two types of mechanisms of water absorption. One mechanism attains the total surface area of the multilayered film based on the B.E.T. method; the other method is that the micropores are completely filled when the gas pressure is greater than the critical value and form capillary shaped condensation. Assuming the micropores are cylindrical, Wheele's formula can be written in the following form:

$$V_0 - V = \pi \int_{R+t}^{\infty} (r - t)^2 L(r) dr, \quad (1)$$

In the formula, V_o and V separately represent saturated gas pressure p_o and the volume of absorption water steam when in a changing gas pressure p; L(r)dr is the total length of the micropore radius in the r to r + dr range; t is the thickness of the absorption multilayered thin film when the gas pressure is p; and R is the Kelvin radius which acts as the gas pressure ratio p/p_o function. Its expression is

$$R = -\frac{1}{2.303} \cdot \frac{2vr}{R_g T \log_{10}(p/p_0)}. \qquad (2)$$

We can obtain the thickness of the multilayered film from the Wheele-Halsey [7] formula

$$t = 3.23 \left\{ \frac{5}{2.303 \log_{10}(p_0/p)} \right\}^{1/3}, \qquad (3)$$

In the formula, the constant 3.23 is selected according to the hexagonally shaped aggregation molecules.

Distribution function L(r) of the micropores and inner surface area which can use p_o/p as the function measure the absorption water steam volume V (see reference [7].

The volume of absorption water can be measured with a QSG20 quartz crystal microbalance from the Balzers Company. In reality, it is measured by the sedimentation or absorption qualitative transformation on the surface which are frequency changes. See fig. 7 for the single layer film water absorption isothermal line and the micropore size distribution.

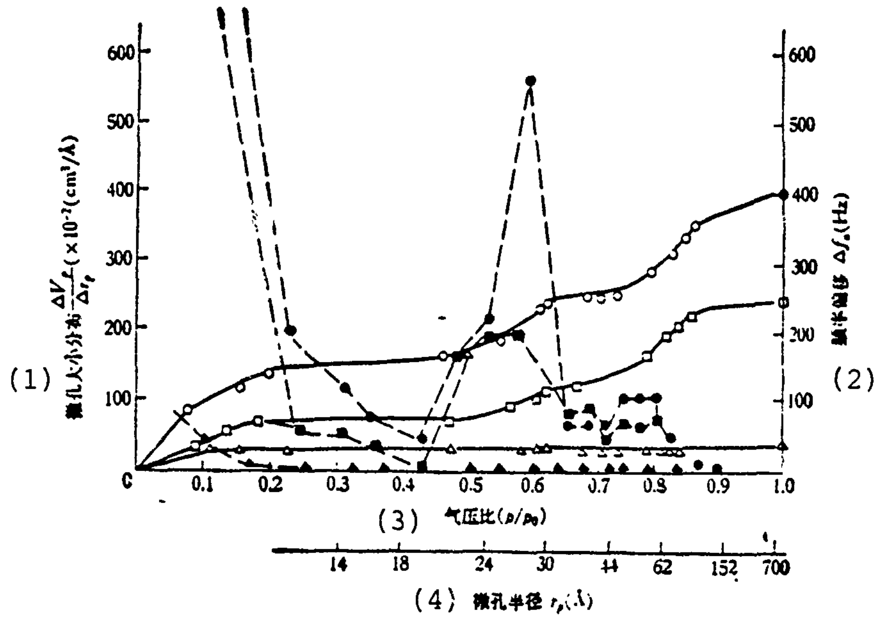

Fig. 7 Single Layer Film Water Absorption Isothermal Line and Micropore Size Distribution

Key: 1. Micropore size distribution
2. Frequency shift
3. Gas pressure ratio
4. Micropore radius

p/p_o is the absorption water change of the gas pressure saturation and the gas pressure ratio; r_p is the micropore radius (Å); $\Delta V_p/\Delta r_p$ is the micropore size distribution; Δf_n is the frequency shift. In the figure the symbols 0, □ and Δ are the isothermal lines of three different material thin films: M_gF_2, Na_3AIF_6 and ZnS

It is necessary to explain here that after finding the film layer's "columnar body + hole" people have perceptual cognition yet the way to consider the characteristics of the thin film within a quantitative formulation so as to meet the demands of film system design and thus improve the film system's

structure is the task of film layer structural design. Therefore, the total surface area of the crystal in the thin film as well as the size of the micropores are essential parameters. In foreign countries today they have already begun to carry out work in this area. For example, Ritter of the Balzers Company has measured the filling density of 13 medium thin films. Any thin film during the steam plating process or after plating only requires a filling density of P to produce changes and the refracting power of the thin film changes with it. The optical characteristics of the film layer or film system also changes with it. Therefore, the changes of the filling density directly influence the optical characteristics and the filling density and size of the micropores are closely related.

See table 1 for the filling densities of commonly used medium thin films.

(1) 材料	(2) 填充密度 P（基片温度 T℃）
Na_3AlF_6	0.88(30);0.98(190)
MgF_2	0.72(30);0.96(330)
CaF_2	0.57(30)
AlF_3	0.64(30)
LaF_3	0.80(30)
NaF_3	0.80(30)
PbF_2	0.91(30)
SiO_2	0.90(30)
Al_2O_3	1.00(30)
ZrO_2	0.67(30)
ZnS	[illegible]
ZnSe	[illegible]

Table 1

Key: 1. Material
2. Filling density P (substrate temperature T^{o}C)

The filling density P expresses the hole level in the thin

film, that is, P=thin film density/block material density

$$\rho = (n_f^2 - 1)/(n_f^2 + 1) \cdot (n_m^2 + 2)/(n_m^2 - 1) \qquad (4)$$

In the formula, n_f and n_m are separately the refracting powers of the thin film and large block material.

Guenther [3] used an electron microscope to photograph the cross section of a 23 layer $\lambda/4$ ZnS-MgF_2 film system. Medium thin film is composed of numberless columnar bodies and there are micropores between the columnar bodies. Most of the sections of the columnar bodies are circular and when measuring the columnar body radii of TiO_2, ZnS and MgF_2 film, their statistical results coincide with the Poisson equation (see table 2).

(1) 薄膜	(2) 柱状体直径 (nm) (平均值)	标准偏差 (3)
TiO_2	19.8	6.6
ZnS	27.6	11.3
MgF_2	27.2	9.0

Table 2

Key: 1. Thin film
2. Columnar body radius (nm) (mean value)
3. Standard Deviation

The reason for the formation of columnar bodies has still not been thoroughly explained. Some consider that there is a close relation between the thin film formation process and substrate temperature. In 1967, Drift carried out theoretical analysis on the longitudinal growth of crystals [9]. His work

has considerable reference value for the study of structural crystallography.

However, works by several of the above mentioned scholars have not given serious attention to the problem of selecting the superior columnar body structure.

It is not accidental that the topic of the 1978 Fourth International Thin Films Conference [10] was "The Structural Quality of Thin Films." It shows that since 1970 research on thin film structure has become a major concern of thin film work in each country.

III. Concluding Remarks

In less than 10 years, from the attaining of electron micrographs of multilayered film system cross sections to date, although much research is currently being done and important advances are being gained, there are nevertheless still many problems. For example, the effects of crystal growth, film layer stress, filling gas types and absorption states on multilayered optical film systems and other thin film structures as well as the relationship of the thin film 's mechanical strength, adhesive force and chemical stability with the thin film structure are all topics worthy of in-depth research. The anti-laser damage of thin film is closely related to the film's structure.

The technique most often used at present for making thin film is still the vacuum evaporation method. The application of this technique is quite wide, technical conditions are relatively mature and thus it has become a traditional technique. Yet, there are noticeable drawbacks in the area of thin film structure. That is, the quality is relatively remiss, adhesive force is weak and there are many internal spaces. Naturally, there are also the

objective conditions of humidity and activation gas permeation. Under these conditions, a cathode sputtering technique which has not been used for years is being revitalized and accompanying it are radio frequency ion sputtering and magnetic control sputtering. The most outstanding features of these new techniques is that the energy of the sputtered material spattered towards the substrate is far greater than that of the evaporation molecules. As a result, the adhesive force must be stronger and the film layer structure is more compact. The former problem of the sputtering speed not being high is being resolved. Aside from metallic film, medium thin film can also be sputtered. This shows that research on solid thin film structures is in a very lively and vigorous stage.

References

[1] D.W. Pashly, J. Vac.Sci. and Tech.,3(1966). 156-167.

[2] C.W.B. Grigson and D.B. Dove. J. Vac. Sci. and Tech. 3(1966). 120.

[3] J.M. Pearson. Thin Solid Films. 6(1970). 349-358.

[4] H.A. MacLeod and D.Richmond. Thin Solid Films. 37(1976). 163-169.

[5] A. Van der Drift, Philips. Res. Rept. 21(1966). 289-303.

[6] S. Ogura and H.A. MacLeod. Thin Solid Films. 37(2976). 163-169.

[7] S.J. Grigg and K.S.W. Sing, Adsorption Surface Area and Porosity, Academic Press, London. (1967). 135.

[8] K.H. Guenther. Appl. Opt., 15(1976). 2992.

[9] A. Van der Drift, Phillips. Res. Rept. 22(1967). 267-288.

[10] Thin Solid Films. 57-2(1979); Thin Solid Films. 58-1(1979).